Computer Assisted Mechanics and Engineering Sciences, 4: 587–605, 1997.
Copyright © 1997 by Polska Akademia Nauk

Hybrid-equilibrium elements with control of spurious kinematic modes

Edward Anthony Ward Maunder
School of Engineering, University of Exeter, Exeter, EX44QF, England

José Paulo Moitiniho de Almeida
Instituto Superior Tecnico, Technical University of Lisbon,
Avenue Rovisco Pais, 1096 Lisboa Codex, Portugal

(Received December 20, 1996)

A review is presented of a recent formulation of hybrid-equilibrium elements for modelling planar structural problems. The formulation is based on the use of polynomials of general degree to approximate internal stress fields and bounding side displacements. The existence of hyperstatic stress fields and spurious kinematic modes are considered algebraically for both primitive and macro-elements, the latter providing a means of controlling or removing the spurious modes in the former. Consideration is given to stress fields which are statically admissible, and to Trefftz stress fields which are both statically and kinematically admissible.

1. Introduction

The potential advantages of stress based elements, such as hybrid-equilibrium elements, have long been recognized [1, 2, 4, 7, 10, 11]. In particular these elements offer to the designer the prospect of using solutions for stress which satisfy strong equilibrium conditions throughout the structure. For such a solution the stress field must (a) satisfy the differential equations of equilibrium within each element, and (b) equilibrate with codiffusive tractions between elements or applied to the boundary of the structure. Solutions of this nature are not generally produced by conventional finite element procedures based on displacement fields.

However computational models formed from hybrid-equilibrium elements may carry the penalty of being unstable for certain patterns of loading due to the presence of spurious kinematic modes or "mechanisms". The existence of such modes depends on the geometry of the mesh, and the nature of the hybrid fields, e.g. the degree and completeness of polynomial fields, and the kinematical admissibility of the stress fields. In the case of Trefftz stress fields the conditions for kinematical admissibility are automatically satisfied.

Alternative techniques for addressing potential problems with these modes exist, and they include (i) the use of "smart" algorithms for the solution of the algebraic equations for the model when the equations are consistent but dependent [7], (ii) the adoption of hybrid fields for elements which have the effect of removing the spurious modes from them [10, 11], and (iii) the combination of subassemblies of elements into macro-elements in which spurious kinematic modes are absent or are entirely self-contained [1, 5]. It is not yet clear which is the optimum technique but some drawbacks can be identified. For example the equations in (i) may become highly ill-conditioned and yield unrealistic displacements notwithstanding reasonable stress fields; the definition of hybrid fields suitable for (ii) may simply be achieved by increasing the number of internal stress parameters and/or reducing the number of side displacement parameters, however this is likely to lead to a weakening of equilibrium at the element interfaces.

This paper presents a review of recent collaborative research studies into the properties of macro-elements in technique (iii) in the context of 2-D planar structures modelled with hybrid-equilibrium membrane elements. Earlier numerical studies were reported in [5], and the more recent studies reported in this paper are intended to provide an algebraic approach to establish in a more general way the static and kinematic properties of both triangular primitive elements, and macro-elements built from them, using polynomial forms of hybrid fields. In Section 2 a general formulation of triangular primitive elements is considered with vector spaces of stress and displacement fields, including Trefftz stress fields in a special subspace. The duality of pairs of vector spaces is recognized, and an equilibrium homomorphism is used to establish the existence of hyperstatic stress fields and spurious kinematic modes. This is followed in Section 3 by an analysis of macro-elements formed from triangular primitive elements connected together with one common internal geometric node point. Some general properties are established by considering the rank of a statical matrix, in algebraic form, which expresses the equilibrium and admissibility conditions for interface tractions between the primitives.

2. Triangular primitive elements

2.1. General formulation of stress based hybrid elements

For the hybrid element statically admissible stress fields $\boldsymbol{\sigma}$ and boundary displacements $\boldsymbol{\delta}$ will be defined independently within the element and on each side respectively as in the formulation in [7]. These fields are expressed in Equation (1)

$$\{\boldsymbol{\sigma}\} = [\mathbf{S}]\,\{\mathbf{s}\}\ , \qquad \text{and} \qquad \{\boldsymbol{\delta}\} = [\mathbf{V}]\,\{\mathbf{v}\}\ . \tag{1}$$

The columns of $[\mathbf{S}]$ and $[\mathbf{V}]$ are independent and number n_{s} and n_{v}. It is assumed that although the sides are free to deform independently of each other, the columns of $[\mathbf{V}]$ span all three rigid body modes of the element. On the element boundary stress $\{\boldsymbol{\sigma}\}$ is equilibrated by tractions $\{\mathbf{t}\}=[\mathbf{N}]\{\boldsymbol{\sigma}\}$ which leads to the work product on the boundary expressed in Equation (2):

$$\oint \{\boldsymbol{\delta}\}^{\mathrm{T}}\,\{\mathbf{t}\}\,\mathrm{d}\Gamma = \{\mathbf{v}\}^{\mathrm{T}}\,[\mathbf{D}]\,\{\mathbf{s}\} = \{\mathbf{s}\}^{\mathrm{T}}\,[\mathbf{D}]^{\mathrm{T}}\,\{\mathbf{v}\} = \{\mathbf{v}\}^{\mathrm{T}}\,\{\mathbf{g}\} = \{\mathbf{s}\}^{\mathrm{T}}\,\{\boldsymbol{\varepsilon}\}\ , \tag{2}$$

where $[\mathbf{D}] = \oint [\mathbf{V}]^{\mathrm{T}}\,[\mathbf{NS}]\,\mathrm{d}\Gamma$ and where:

$$\{\mathbf{g}\} = [\mathbf{D}]\,\{\mathbf{s}\}\ , \tag{3}$$

and:

$$\{\boldsymbol{\varepsilon}\} = [\mathbf{D}]^{\mathrm{T}}\,\{\mathbf{v}\}\ . \tag{4}$$

This scalar work product means that vectors $\{\mathbf{g}\}$ and $\{\boldsymbol{\varepsilon}\}$ represent generalised side tractions and internal deformations which belong to vector spaces dual to those represented by $\{\mathbf{v}\}$ and $\{\mathbf{s}\}$ respectively. Equations (3) and (4) can be considered as generalised equilibrium and compatibility equations for an element, with the generalised constitutive relations provided by the natural flexibility matrix $[\mathbf{F}]$ in Equation (5).

$$[\mathbf{F}]\,\{\mathbf{s}\} = \{\boldsymbol{\varepsilon}\}\ , \qquad \text{where} \qquad [\mathbf{F}] = \int [\mathbf{S}]^{\mathrm{T}}\,[\mathbf{f}]\,[\mathbf{S}]\,\mathrm{d}\Omega, \tag{5}$$

and $[\mathbf{f}]$ transforms stress to strain.

$[\mathbf{D}]$ has dimensions $n_{\mathrm{v}} \times n_{\mathrm{s}}$ and is a key matrix for the hybrid element. $\{\mathbf{v}\}$ is a spurious kinematic mode or "mechanism" when it corresponds to zero deformation in Equation (4) without being a rigid body mode. Such a mode, denoted by $\{\mathbf{v}_{\mathrm{skm}}\}$, belongs to the nullspace of $[\mathbf{D}]^{\mathrm{T}}$, does zero

work for all stress fields within the element, and has zero corresponding stress from Equation (5). The number of spurious kinematic modes, n_{skm}, is given by Equation (6):

$$n_{\text{skm}} = n_{\text{v}} - 3 - \text{rank}\,[\mathbf{D}]\ . \tag{6}$$

$\{\mathbf{s}\}$ represents a hyperstatic stress mode, denoted by $\{\mathbf{s}_{\text{hyp}}\}$, when it produces zero generalised tractions in Equation (3). Such a mode belongs to the nullspace of $[\mathbf{D}]$, and does zero work for all displacements of the sides of the element. The number of hyperstatic modes, n_{hyp}, is given by Equation (7):

$$n_{\text{hyp}} = n_{\text{s}} - \text{rank}\,[\mathbf{D}]\ . \tag{7}$$

Combining Equations (6) and (7) gives a simple relation between the numbers of the two types of modes:

$$n_{\text{skm}} = (n_{\text{v}} - 3) - n_{\text{s}} + n_{\text{hyp}}\,. \tag{8}$$

The rank$[\mathbf{D}]$ has been studied numerically [9], e.g. using singular value decomposition, but in certain cases more general results can be derived in algebraic form. Before considering the properties of primitive or macro-elements, the general structures of the vector spaces formed from polynomial stress fields are reviewed.

2.2. Polynomial stress fields for membrane elements

Using vector space concepts, the complete polynomials of degree p, with reference to some set of possibly oblique linear axes, form a stress space $\boldsymbol{\Sigma}^p$ of dimension $1.5(p+1)(p+2)$ for plane stress problems. It will be convenient to decompose the spaces into direct sums of subspaces $\boldsymbol{\Sigma}^{np}$, each of which contains stress components all of the same degree n $(0 \le n \le p)$, i.e.

$$\boldsymbol{\Sigma}^p = \boldsymbol{\Sigma}^{0p} \oplus \boldsymbol{\Sigma}^{1p} \oplus \ldots \oplus \boldsymbol{\Sigma}^{np} \oplus \ldots \oplus \boldsymbol{\Sigma}^{pp}.$$

The stress components of $\boldsymbol{\Sigma}^{np}$ have the form:

$$\left\{\begin{array}{c}\sigma_x\\ \sigma_y\\ \tau\end{array}\right\} = \left\{\begin{array}{l} a_1x^n + a_2x^{n-1}y + a_3x^{n-2}y^2 + \ \ldots\ + a_nxy^{n-1} + a_{n+1}y^n \\ b_1x^n + b_2x^{n-1}y + b_3x^{n-2}y^2 + \ \ldots\ + b_nxy^{n-1} + b_{n+1}y^n \\ c_1x^n + c_2x^{n-1}y + c_3x^{n-2}y^2 + \ \ldots\ + c_nxy^{n-1} + c_{n+1}y^n \end{array}\right\} \tag{9}$$

and the dimension of $\boldsymbol{\Sigma}^{np}$ is clearly $3(n+1)$.

2.2.1. *Statically admissible subspaces*

In this subspace of $\boldsymbol{\Sigma}^p$ the stresses must satisfy equilibrium with zero body forces, i.e. $\text{div}\,\boldsymbol{\sigma} = \mathbf{0}$. When $\boldsymbol{\sigma}$ belongs to $\boldsymbol{\Sigma}^{np}$ and Equation (9) describes contravariant components as in Figure 1 for example, the vector $\text{div}\,\boldsymbol{\sigma}$ is related by a non-singular transformation to:

$$\left\{\begin{array}{c}\dfrac{\partial\sigma_x}{\partial x} + \dfrac{\partial\tau}{\partial y}\\[2ex] \dfrac{\partial\sigma_y}{\partial y} + \dfrac{\partial\tau}{\partial x}\end{array}\right\} = \left\{\begin{array}{l}(na_1 + c_2)\,x^{n-1} + ((n-1)\,a_2 + 2c_3)\,x^{n-2}y + \ldots + (a_n + nc_{n+1})y^{n-1}\\ (b_2 + nc_1)\,x^{n-1} + (2b_3 + (n-1)\,c_2)\,x^{n-2}y + \ldots + (nb_{n+1} + c_n)y^{n-1}\end{array}\right\}. \tag{10}$$

When $\text{div}\,\boldsymbol{\sigma} = \mathbf{0}$ at all points x, y all the $2n$ coefficients in Equation (10) must be zero for each value of n. This gives rise to $2n$ equations which relate the coefficients:

$$(n-i+1)\,a_i + (i)\,c_{i+1} = 0; \quad (i)\,b_{i+1} + (n-i+1)\,c_i = 0 \qquad i = 1, \ldots, n. \tag{11}$$

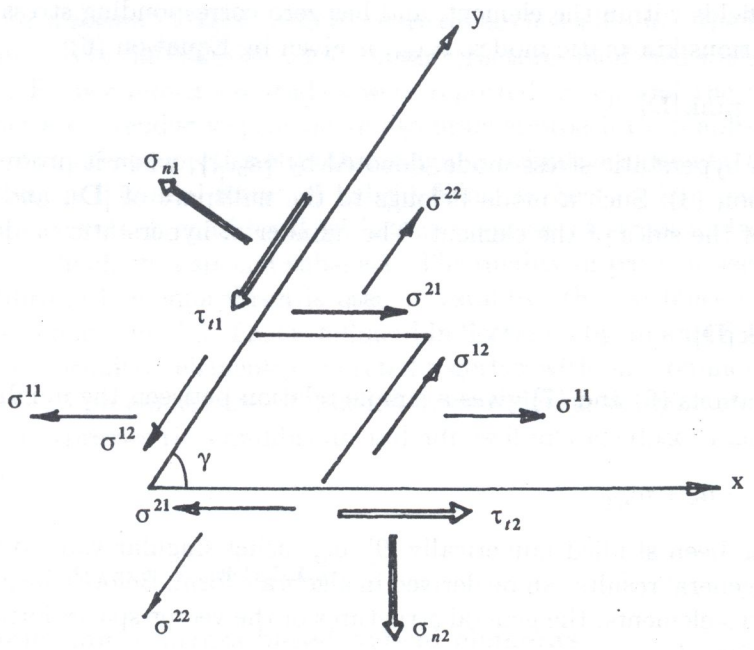

Fig. 1. Stress components at an oblique corner

$3(n+1)-2n=(n+3)$ independent coefficients can be selected as b_1, c_1 to c_{n+1}, and a_{n+1}. These coefficients generate the subspace $\boldsymbol{\Sigma}^{np}_{\mathrm{SA}}$ of $\boldsymbol{\Sigma}^{np}$ which has dimension $(n+3)$. Thus the space of statically admissible stress fields $\boldsymbol{\Sigma}^{p}_{\mathrm{SA}}$ is the direct sum:

$$\boldsymbol{\Sigma}^{p}_{\mathrm{SA}} = \boldsymbol{\Sigma}^{0p}_{\mathrm{SA}} \oplus \boldsymbol{\Sigma}^{1p}_{\mathrm{SA}} \oplus \ldots \oplus \boldsymbol{\Sigma}^{np}_{\mathrm{SA}} \oplus \ldots \oplus \boldsymbol{\Sigma}^{pp}_{\mathrm{SA}},$$

and $\boldsymbol{\Sigma}^{p}_{\mathrm{SA}}$ has dimension

$$\sum_{n=0}^{n=p} (n+3) = \frac{1}{2}(p+1)(p+6).$$

2.2.2. Statically and kinematically admissible subspaces — Trefftz stress fields

Each subspace $\boldsymbol{\Sigma}^{np}_{\mathrm{SA}}$ contains a subspace of stress fields whose strains derived from the constitutive relations embodied in [**f**] are compatible, e.g. for homogeneous isotropic material the stresses must also satisfy $\nabla^2(\sigma_1+\sigma_2)=0$, where σ_1 and σ_2 are the principal stresses, at each point. Assuming such material and the use of orthogonal cartesian axes for simplicity, the stress fields from $\boldsymbol{\Sigma}^{np}_{\mathrm{SA}}$ give:

$$(\sigma_1+\sigma_2) = (\sigma_x+\sigma_y) = \sum_{i=1}^{n+1} (a_i+b_i)\, x^{n-i+1} y^{i-1},$$

and then

$$\begin{aligned}\nabla^2(\sigma_x+\sigma_y) = {} & [n(n-1)(a_1+b_1)+2(a_3+b_3)]\, x^{n-2} \\ & +[(n-1)(n-2)(a_2+b_2)+6(a_4+b_4)]\, x^{n-3}y+\ldots \\ & +[2(a_{n-1}+b_{n-1})+n(n-1)(a_{n+1}+b_{n+1})]\, y^{n-2}. \end{aligned} \tag{12}$$

For the compatibility condition to hold at all points x, y it is required that each of the $(n-1)$ coefficients in Equation (12) be zero for all $n \geq 2$, i.e. there are $(n-1)$ independent relations

between the $(n+3)$ independent coefficients b_1, c_1 to c_{n+1}, and a_{n+1}. This leaves 4 independent coefficients (e.g. b_1, c_1, and c_{n+1}, a_{n+1}) for each value of $n \geq 2$, and the dimension of the Trefftz subspace $\boldsymbol{\Sigma}_{\mathrm{TR}}^{np}$ is 4. For $n = 0$ or 1 the statically admissible stress fields are all compatible and then $\boldsymbol{\Sigma}_{\mathrm{TR}}^{np} = \boldsymbol{\Sigma}_{\mathrm{SA}}^{np}$. Thus the space of Trefftz stress fields $\boldsymbol{\Sigma}_{\mathrm{TR}}^{p}$ is the direct sum:

$$\boldsymbol{\Sigma}_{\mathrm{TR}}^{p} = \boldsymbol{\Sigma}_{\mathrm{TR}}^{0p} \oplus \boldsymbol{\Sigma}_{\mathrm{TR}}^{1p} \oplus \ldots \oplus \boldsymbol{\Sigma}_{\mathrm{TR}}^{np} \oplus \ldots \oplus \boldsymbol{\Sigma}_{\mathrm{TR}}^{pp},$$

and $\boldsymbol{\Sigma}_{\mathrm{TR}}^{p}$ has dimension

$$3 + 4 + \sum_{n=2}^{n=p} 4 = (3 + 4p).$$

For the case of orthogonal axes the dependent stress coefficients c_2 to c_n are given explicitly by the following simple matrix equations in terms of the 4 independent coefficients [6]:

for n odd

$$\begin{Bmatrix} c_2 \\ \vdots \\ c_j \\ \vdots \\ c_n \end{Bmatrix} = [\mathbf{C}_{\mathrm{odd}}^{n}] \begin{bmatrix} \frac{1}{n+1} & 0 & 0 & 0 \\ 0 & \frac{1}{n+1} & 0 & 0 \\ 0 & 0 & \frac{1}{n+1} & 0 \\ 0 & 0 & 0 & \frac{1}{n+1} \end{bmatrix} \begin{Bmatrix} b_1 \\ c_1 \\ c_{n+1} \\ a_{n+1} \end{Bmatrix}, \tag{13}$$

where

$$[\mathbf{C}_{\mathrm{odd}}^{n}] =$$

$$\left[\begin{array}{cc|cc} (n-1)\ {}_nC_{n-1} & 0 & (-1)^{\frac{n-1}{2}}\ 2\ {}_nC_1 & 0 \\ 0 & -(n-1)\ {}_nC_{n-2} & 0 & (-1)^{\frac{n-3}{2}}\ 2\ {}_nC_2 \\ -(n-3)\ {}_nC_{n-3} & 0 & (-1)^{\frac{n-3}{2}}\ 4\ {}_nC_3 & 0 \\ 0 & (n-3)\ {}_nC_{n-4} & 0 & (-1)^{\frac{n-5}{2}}\ 4\ {}_nC_4 \\ \vdots & \vdots & \vdots & \vdots \\ (-1)^{\frac{j-3}{2}}\ (n+2-j)\ {}_nC_{n+2-j} & 0 & (-1)^{\frac{n+2-j}{2}}\ (j-1)\ {}_nC_{j-2} & 0 \\ 0 & (-1)^{\frac{j-1}{2}}\ (n+2-j)\ {}_nC_{n+1-j} & 0 & (-1)^{\frac{n-j}{2}}\ (j-1)\ {}_nC_{j-1} \\ \vdots & \vdots & \vdots & \vdots \\ (-1)^{\frac{n-5}{2}}\ 4\ {}_nC_4 & 0 & (n-3)\ {}_nC_{n-4} & 0 \\ 0 & (-1)^{\frac{n-3}{2}}\ 4\ {}_nC_3 & 0 & -(n-3)\ {}_nC_{n-3} \\ (-1)^{\frac{n-3}{2}}\ 2\ {}_nC_2 & 0 & -(n-1)\ {}_nC_{n-2} & 0 \\ 0 & (-1)^{\frac{n-1}{2}}\ 2\ {}_nC_1 & 0 & (n-1)\ {}_nC_{n-1} \end{array}\right]$$

and for n even

$$\begin{Bmatrix} c_2 \\ \vdots \\ c_j \\ \vdots \\ c_n \end{Bmatrix} = [C_{\mathrm{even}}^{n}] \begin{bmatrix} \frac{1}{n+2} & & & \\ & \frac{1}{n} & & \\ & & \frac{1}{n} & \\ & & & \frac{1}{n+2} \end{bmatrix} \begin{Bmatrix} b_1 \\ c_1 \\ c_{n+1} \\ a_{n+1} \end{Bmatrix}, \tag{14}$$

where

$[\mathbf{C}^n_{\text{even}}] =$

$$\left[\begin{array}{cc|cc}
n\ {}_nC_{n-1} & 0 & 0 & (-1)^{\frac{n-2}{2}}\ 2\ {}_nC_1 \\
0 & -(n-2)\ {}_nC_{n-2} & (-1)^{\frac{n-2}{2}}\ 2\ {}_nC_2 & 0 \\
-(n-2)\ {}_nC_{n-3} & 0 & 0 & (-1)^{\frac{n-4}{2}}\ 4\ {}_nC_3 \\
0 & (n-4)\ {}_nC_{n-4} & (-1)^{\frac{n-4}{2}}\ 4\ {}_nC_4 & 0 \\
\vdots & \vdots & \vdots & \vdots \\
0 & (-1)^{\frac{j-2}{2}}\ (n+2-j)\ {}_nC_{n+2-j} & (-1)^{\frac{n+2-j}{2}}\ (j-2)\ {}_nC_{j-2} & 0 \\
(-1)^{\frac{j-2}{2}}\ (n+2-j)\ {}_nC_{n+1-j} & 0 & 0 & (-1)^{\frac{n-j}{2}}\ j\ {}_nC_{j-1} \\
\vdots & \vdots & \vdots & \vdots \\
0 & (-1)^{\frac{n-4}{2}}\ 4\ {}_nC_4 & (n-4)\ {}_nC_{n-4} & 0 \\
(-1)^{\frac{n-4}{2}}\ 4\ {}_nC_3 & 0 & 0 & -(n-2)\ {}_nC_{n-3} \\
0 & (-1)^{\frac{n-2}{2}}\ 2\ {}_nC_2 & -(n-2)\ {}_nC_{n-2} & 0 \\
(-1)^{\frac{n-2}{2}}\ 2\ {}_nC_1 & 0 & 0 & n\ {}_nC_{n-1}
\end{array}\right].$$

In matrices $[\mathbf{C}^n_{\text{odd}}]$, and $[\mathbf{C}^n_{\text{even}}]$ terms such as ${}_nC_j$ represent the binomial coefficients, i.e. ${}_nC_j = \dfrac{n!}{j!\,(n-j)!}$. The remaining dependent coefficients a_1 to a_n, and b_2 to b_{n+1} are defined by the Equation (11). This direct generation of Trefftz stress fields by Equations (11), (13), and (14) is an alternative to the more usual, but indirect, generation via the formation of Airy stress functions which satisfy the biharmonic compatibility equation [3].

2.3. Polynomial displacement and traction fields on the sides of a primitive triangle

Hybrid equilibrium elements require the definition of both internal stress fields and displacement fields on the boundaries of the elements. The displacements are defined independently and separately on each side of an element, and form the space Δ^p with typical vector $\mathbf{v}$ when based on complete polynomials of degree p. This space then has the dimension $3 \times 2(p+1) = 6(p+1)$. The use of displacements of the same degree p as the stress fields is intended to lead to continuity of normal and tangential stresses between elements, and hence to complete equilibrium. However this desirable result can be frustrated by the presence of spurious kinematic modes in the primitive elements.

Dual to the space Δ^p there is the space of side tractions $\mathbf{G}^p$ with typical vector denoted by $\mathbf{g}$. Two subspaces of $\mathbf{G}^p$ are defined: $\mathbf{G}^p_{\text{E}}$ and $\mathbf{G}^p_{\text{CE}}$. $\mathbf{G}^p_{\text{E}}$ consists of those vectors $\mathbf{g}$ which satisfy three independent global equilibrium conditions for an element. This subspace thus has dimension $6(p+1) - 3 = 3(2p+1)$. $\mathbf{G}^p_{\text{CE}}$ is a subspace of $\mathbf{G}^p_{\text{E}}$ and contains tractions which satisfy not only global equilibrium, but also three local equilibrium conditions at the three corners of a triangular element. These conditions can be expressed in a variety of ways depending on the choice of axes or stress components. However what they express is the local rotational equilibrium associated with an infinitesimal element at a corner of a finite element — this is equivalent to the usual concept of complementary shear stresses. With reference to Figure 1 this can be expressed in terms of local contravariant stress components σ^{ij} or local normal and tangential traction components:

$$\sigma^{12} - \sigma^{21} = 0, \qquad \text{or} \qquad (\tau_{t1} + \tau_{t2}) - (\sigma_{n1} - \sigma_{n2}) \cot \gamma = 0. \tag{15}$$

It is clear that tractions belonging to $\mathbf{G}^p_{\text{CE}}$ define single valued stress states within the corners of an element.

2.4. Equilibrium homomorphism of Σ^p_{SA} onto G^p_{CE} for a primitive triangle

A homomorphism e is defined by taking the image of a statically admissible stress field $\boldsymbol{\sigma}$ as the boundary tractions $\mathbf{g}$ which are in equilibrium with the stress field:

$$e : \Sigma^p_{SA} \rightarrow G^p_{CE} . \tag{16}$$

Clearly this mapping is "into" since all statically admissible stress fields have equilibrating tractions which must satisfy all the global and local corner equilibrium conditions. What is not so obvious is that the mapping is "onto" [6], i.e. every traction $\mathbf{g} \in G^p_{CE}$ has at least one stress field $\boldsymbol{\sigma} \in \Sigma^p_{SA}$ as an inverse image. An important consequence of this mapping being "onto" concerns the dimension of the space of hyperstatic stress fields Σ^p_{HS} when element stress fields are defined to span Σ^p_{SA}. When the boundary displacements belong to the complete space of polynomials of degree p the hyperstatic stress fields represented by $\{\mathbf{s}\}$ in Equation (1) have zero tractions on the element boundary and then n_{hyp} = dimension Σ^p_{HS} = dimension Σ^p_{SA} - dimension G^p_{CE}.

Dimension G^p_{CE} is found to be dependent on the value of p [6], and it can be simply determined from the rank[$\mathbf{A}$], where matrix [$\mathbf{A}$] represents the projection of G^p_E onto its quotient space G^p_E/G^p_{CE} i.e. dimension G^p_{CE} = dimension G^p_E – rank [$\mathbf{A}$]. [$\mathbf{A}$] can be constructed as a $3 \times 3(2p+1)$ matrix with coefficient a_{ij} equal to the left hand side of Equation (15) for corner i and traction distribution j from a basis for G^p_E. In [6] it is shown that rank[$\mathbf{A}$] = 0, 2, or 3 when $p = 0, 1$, or ≥ 2 respectively, and consequently dimension $G^p_{CE} = 3, 7$, or $6p$ for the respective values of p.

2.4.1. Hyperstatic stress fields for triangular equilibrium elements

The mapping e is an isomorphism when $p \leq 3$ and then $n_{hyp} = 0$, whereas e is an homomorphism for $p \geq 4$ and then $n_{hyp} = 0.5\,(p+1)\,(p+6) - 6p = 0.5\,(p-2)\,(p-3)$. The single hyperstatic stress field when $p = 4$ is a combination of stress fields from Σ^2_{SA}, Σ^3_{SA}, and Σ^4_{SA}, and is defined in terms of the oblique axes of Figure 2 in Equation (17).

$$\{\boldsymbol{\sigma}\} = -\left\{ \begin{array}{c} -\dfrac{x^2}{3} + \dfrac{2x^3}{3b} + \dfrac{2x^2y}{a} - \dfrac{x^4}{3b^2} - \dfrac{2x^3y}{ab} - \dfrac{2x^2y^2}{a^2} \\ -\dfrac{y^2}{3} + \dfrac{2xy^2}{b} + \dfrac{2y^3}{3a} - \dfrac{2x^2y^2}{b^2} - \dfrac{2xy^3}{ab} - \dfrac{y^4}{3a^2} \\ \dfrac{2xy}{3} - \dfrac{2x^2y}{b} - \dfrac{2xy^2}{a} + \dfrac{4x^3y}{3b^2} + \dfrac{3x^2y^2}{ab} + \dfrac{4xy^3}{3a^2} \end{array} \right\} \tag{17}$$

This stress field is illustrated in Figures 3, 4, and 5, which include a plot of stress trajectories [8] and a simplified "strut and tie" model to aid the visualisation of this mode of self stressing. This mode would be typical of the stress fields arising from differential shrinkage of the material of the element, although it should be noted that this stress field does not belong to Σ^4_{TR} for a linear elastic material.

2.4.2. Hyperstatic stress fields for the triangular Trefftz elements

Using the oblique axes of Figure 2, the oblique traction components on sides 31 and 32 which equilibrate with the general stress field of Equation (9) are defined by:

$$\{\mathbf{t}\} = -\sin\gamma \cdot x^n \left\{ \begin{array}{c} c_1 \\ b_1 \end{array} \right\} \quad \text{on side 31,}$$

$$\{\mathbf{t}\} = -\sin\gamma \cdot y^n \left\{ \begin{array}{c} a_{n+1} \\ c_{n+1} \end{array} \right\} \quad \text{on side 32.}$$

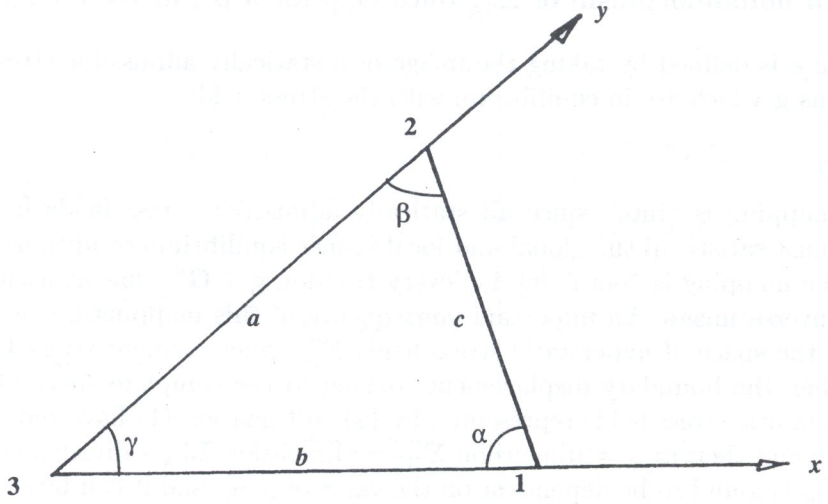

Fig. 2. Local oblique axes for a primitive triangle associated with corner 3

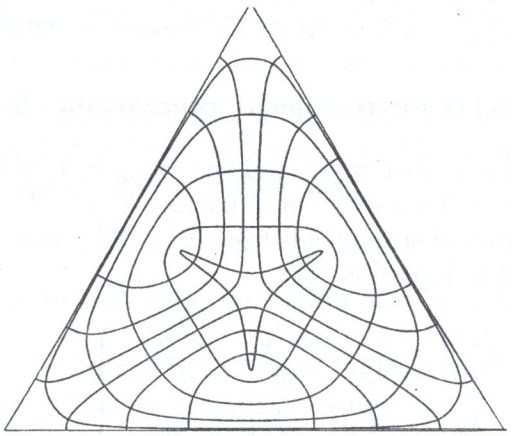

Fig. 3. 4th degree hyperstatic stress mode; stress trajectories

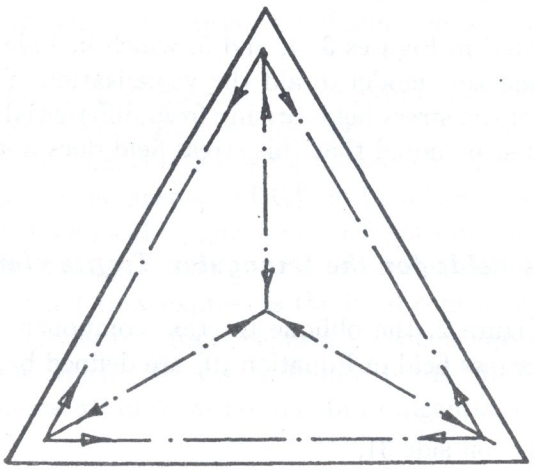

Fig. 4. 4th degree hyperstatic stress mode; simplified strut and tie model

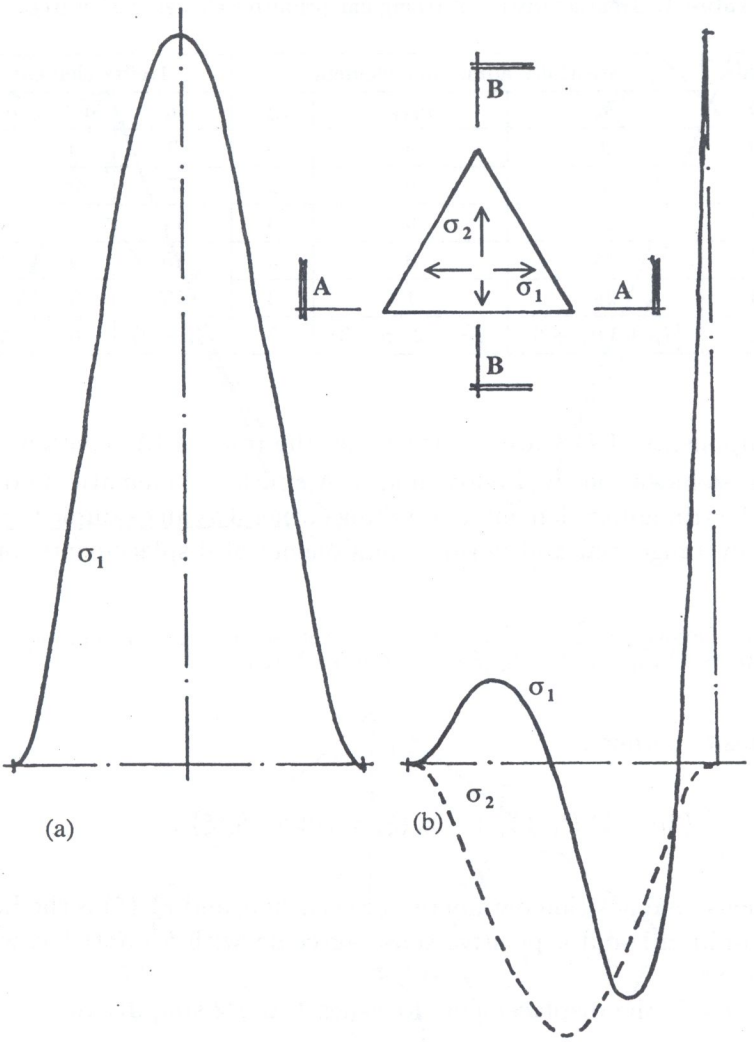

Fig. 5. 4th degree hyperstatic stress mode: distributions of principal stresses on (a) section A-A and (b) section B-B

These tractions are thus functions of the four independent stress coefficients b_1, c_1, c_{n+1}, and a_{n+1} which correspond to a basis for $\boldsymbol{\Sigma}_{\mathrm{TR}}^{np}$. Hence for the Trefftz element to have zero tractions on these two sides implies that these four coefficients are zero for all values of $n > 0$, and consequently the null-space of the mapping $e : \boldsymbol{\Sigma}_{\mathrm{TR}}^{p} \rightarrow \mathbf{G}_{\mathrm{CE}}^{p}$ is just the zero stress field. Thus there are **no** hyperstatic stress fields for the Trefftz polynomial element, and $n_{\mathrm{hyp}} = 0$.

2.5. Spurious kinematic modes for the primitive triangular membrane element

The number of spurious kinematic modes, n_{skm}, is given by Equation (8) and is tabulated for elements with stress fields which are (a) statically admissible, and (b) Trefftz fields for various values of degree p in Table 1.

A spurious kinematic mode $\{\mathbf{v}_{\mathrm{skm}}\}$ does zero work with all tractions belonging to the range of the equilibrium homomorphism e. These tractions are termed "admissible". Thus for the **statically admissible element**:

$$\{\mathbf{v}_{\mathrm{skm}}\}^{\mathrm{T}} \{\mathbf{g}\} = 0 \text{ for all } \mathbf{g} \in \mathbf{G}_{\mathrm{CE}}^{p}, \text{ i.e. for all } \{\mathbf{g}\} \text{ satisfying } [\mathbf{A}]\{\mathbf{g}\} = \{\mathbf{0}\} \tag{18}$$

This implies that, in matrix terms,

$$\{\mathbf{v}_{\mathrm{skm}}\} = [\mathbf{A}]^{\mathrm{T}} \{\mathbf{k}\} \tag{19}$$

Table 1. Characteristics of triangular primitive elements of degree p

Degree	Statically admissible element			Trefftz element		
p	n_s	n_{hyp}	n_{skm}	n_s	n_{hyp}	n_{skm}
0	3	0	0	3	0	0
1	7	0	2	7	0	2
2	12	0	3	11	0	4
3	18	0	3	15	0	6
4	25	1	3	19	0	8
p	$\frac{1}{2}(p+1)(p+6)$	$\frac{1}{2}(p-2)(p-3)$	3	$(4p+3)$	0	$2p$

where the three components of $\{\mathbf{k}\}$ are arbitrary, i.e. the rows of $[\mathbf{A}]$ contain a basis for the null-space of $[\mathbf{D}]^{\mathrm{T}}$ which excludes the rigid body modes. A spurious kinematic mode is thus associated with each corner of the triangular element, and taking corner 3 as an example the spurious kinematic mode is defined [6] by tangential and normal components of displacements, on the side opposite corner 1:

$$\delta_t(\xi) = \frac{1}{a}\left[\sum_{n=0}^{n=p}(2n+1)\,P_n(\xi)\right]; \quad \delta_n(\xi) = -\cot\gamma\cdot\delta_t(\xi) \tag{20}$$

and on the side opposite corner 2:

$$\delta_t(\xi) = \frac{1}{b}\left[\sum_{n=0}^{n=p}(-1)^n(2n+1)\,P_n(\xi)\right]; \quad \delta_n(\xi) = \cot\gamma\cdot\delta_t(\xi)\,, \tag{21}$$

where ξ is a non-dimensional position parameter for each side, and $P_n(\xi)$ is the Legendre polynomial of degree n. ξ has limits ± 1 and a positive sense agreeing with an anticlockwise traversal of the boundary of an element.

In particular, for $p = 1$, the displacements for sides 1 and 2 simplify to:

$$\{\boldsymbol{\delta}\} = \begin{Bmatrix}\delta_n\\ \delta_t\end{Bmatrix} = \frac{1}{a}\begin{Bmatrix}-\cot\gamma\,(1+3\xi)\\ (1+3\xi)\end{Bmatrix} \quad \text{and} \quad \begin{Bmatrix}\delta_n\\ \delta_t\end{Bmatrix} = \frac{1}{b}\begin{Bmatrix}\cot\gamma\,(1-3\xi)\\ (1-3\xi)\end{Bmatrix} \tag{22}$$

respectively, and for $p = 2$, the displacements for the two sides become:

$$\begin{Bmatrix}\delta_n\\ \delta_t\end{Bmatrix} = \frac{3}{2a}\begin{Bmatrix}-\cot\gamma\,(-1+2\xi+5\xi^2)\\ (-1+2\xi+5\xi^2)\end{Bmatrix} \quad \text{and} \quad \begin{Bmatrix}\delta_n\\ \delta_t\end{Bmatrix} = \frac{3}{2b}\begin{Bmatrix}\cot\gamma\,(-1-2\xi+5\xi^2)\\ (-1-2\xi+5\xi^2)\end{Bmatrix} \tag{23}$$

respectively. These two particular examples of spurious kinematic modes for the statically admissible element are illustrated in Figure 6.

3. Macro-elements

Macro-elements are considered as assemblies of $n_\Delta \geq 3$ primitive triangular elements of polynomial degree p sharing a common internal node. An example with $n_\Delta = 5$ is illustrated in Figure 7. The macro-elements can be regarded in the same way as primitives, but the stress fields are now defined in a piecewise sense. Again the rank[$\mathbf{D}$] has been studied numerically [9], but arguments based on the macro assembly as a statically indeterminate system have yielded some general algebraic results for the membrane case. A statical analysis of the macro-element as a system of primitive elements leads to general conclusions regarding the degree of hyperstaticity and the number of spurious kinematic modes.

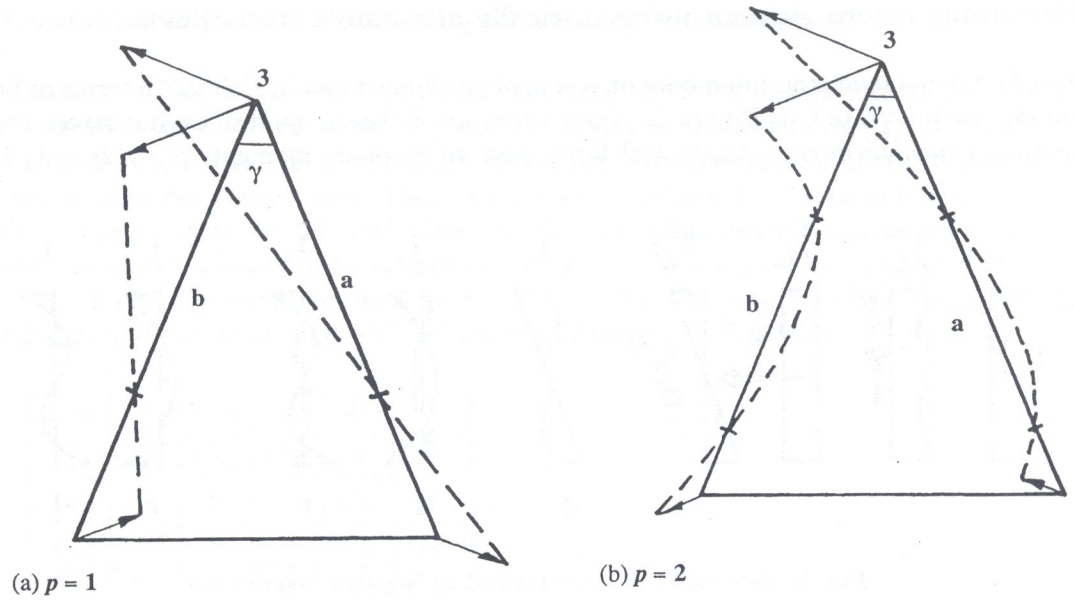

Fig. 6. Spurious kinematic modes for: (a) $p = 1$ and (b) $p = 2$ associated with corner 3

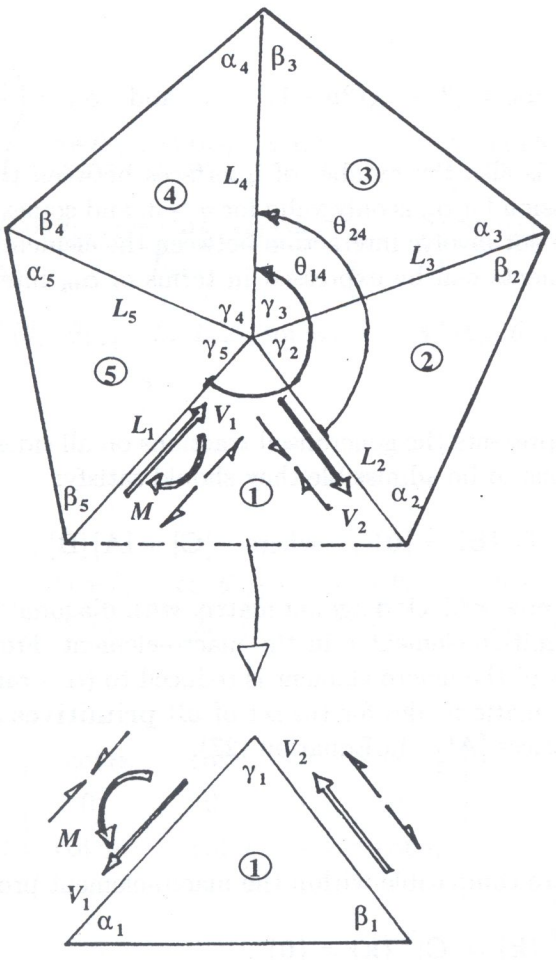

Fig. 7. Notation for a macro-element with $n_\Delta = 5$, including a basis for internal biactions

3.1. Membrane macro-element using statically admissible stress fields

The $2(p+1)$ independent traction modes on a side of an element can be defined in terms of Legendre polynomials as illustrated in Figure 8. Then there are 3 **basic** modes having stress resultants representing a normal force, a tangential force, and an in plane moment, plus $(2p-1)$ **higher-**

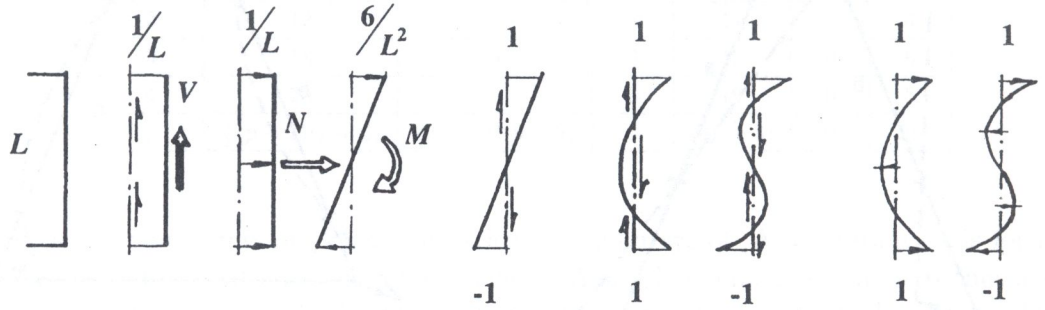

Fig. 8. Side modes of traction based on Legendre polynomials

order or **self-balancing** modes. Leaving aside the question of admissibility for the moment, the assembly of elements would be statically indeterminate of degree α, where α is given by Equation (24).

$$\alpha = \alpha_m + \alpha_p, \quad \text{where} \quad \alpha_m = (3 + n_\Delta(2p-1)) \ , \qquad \text{and} \quad \alpha_p = \left(\frac{n_\Delta}{2}(p-2)(p-3)\right) . \tag{24}$$

n_Δ appears in α_m since it is also the number of interfaces between the primitive elements of the macro-element. The expression for α_p is only valid for $p > 3$, and comes from the hyperstatic modes for the primitives which do not involve interaction between the elements. Self-balanced interactions between the primitive elements can be expressed in terms of α_m internal biactions whose values constitute a vector $\{\mathbf{b}\}$:

$$\{\mathbf{g}\} = [\mathbf{B}]\,\{\mathbf{b}\} \ . \tag{25}$$

In Equation (25) $\{\mathbf{g}\}$ represents the generalised tractions on all sides of all primitives due to the biactions. For these tractions to be admissible they should satisfy:

$$[\mathbf{A}]\,\{\mathbf{g}\} = [\mathbf{A}]\,[\mathbf{B}]\,\{\mathbf{b}\} = [\mathbf{C}]\,\{\mathbf{b}\} = \{\mathbf{0}\} \ , \quad \text{where} \quad [\mathbf{C}] = [\mathbf{A}]\,[\mathbf{B}] \ . \tag{26}$$

In Equation (26) $[\mathbf{A}]$ is now a block diagonal matrix with diagonal submatrices $[\mathbf{A}^e]$ as defined in Section 2.4 for each primitive element e in the macro-element. From the static point of view, the degree of hyperstaticity of the macro-element is reduced to $(\alpha - \text{rank}\,[\mathbf{C}])$. From the kinematic point of view, spurious kinematic modes for the set of **all primitives** are generated by combining the columns of the submatrices $[\mathbf{A}^e]^{\mathrm{T}}$ in Equation (27):

$$\{\mathbf{v}_{\mathrm{skm}}\} = [\mathbf{A}]^{\mathrm{T}}\,\{\mathbf{k}\} \ . \tag{27}$$

These spurious modes are compatible within the macro-element provided that they satisfy:

$$[\mathbf{B}]^{\mathrm{T}}\,\{\mathbf{v}_{\mathrm{skm}}\} = [\mathbf{B}]^{\mathrm{T}}\,[\mathbf{A}]^{\mathrm{T}}\,\{\mathbf{k}\} = [\mathbf{C}]^{\mathrm{T}}\,\{\mathbf{k}\} = \{\mathbf{0}\} \ . \tag{28}$$

Thus the number of spurious modes for the macro-element is given by $(2n_\Delta - \text{rank}\,[\mathbf{C}])$ when $p = 1$, and by $(3n_\Delta - \text{rank}\,[\mathbf{C}])$ when $p \geq 2$. The existence and number of hyperstatic or spurious kinematic modes depends on rank$[\mathbf{C}]$.

3.1.1. Formation of [C] *for a statically admissible macro-element*

[C] has dimensions $3n_\Delta \times \alpha_m$ and it is readily constructed in submatrix format by selecting appropriate bases for the biaction vector $\{\mathbf{b}\}$ and the vector of side tractions $\{\mathbf{g}\}$. [C] is partitioned into submatrices $[\mathbf{C}_{ij}] = [\mathbf{A}^i]\,[\mathbf{B}_{ij}]$ where here i and j refer to the number of the primitive element and the set of biactions respectively. There are 3 basic biactions for the complete macro-element, these will be referred to as set "0"; and there are $(2p-1)$ higher order biactions between each pair of adjacent primitives, these will be referred to as set "j" where j is the number of the interface $(1 \le j \le n_\Delta)$. Thus $[\mathbf{C}_{ij}]$ has dimensions 3×3 or $3\times(2p-1)$. The patterns of submatrices in [B] and [C] are similar, and are illustrated with reference to Figure 7 in Equation (29) when $n_\Delta = 5$.

$$[\mathbf{C}] = \left[\begin{array}{c|c|c|c|c|c} C_{10} & C_{11} & C_{12} & 0 & 0 & 0 \\ \hline C_{20} & 0 & C_{22} & C_{23} & 0 & 0 \\ \hline C_{30} & 0 & 0 & C_{33} & C_{34} & 0 \\ \hline C_{40} & 0 & 0 & 0 & C_{44} & C_{45} \\ \hline C_{50} & C_{51} & 0 & 0 & 0 & C_{55} \end{array}\right]. \tag{29}$$

Using the bases for $\{\mathbf{b}\}$ and $\{\mathbf{g}\}$ as indicated in Figures 7 and 8 with Legendre polynomials, typical submatrices are as follows:

$$[\mathbf{C}_{i0}] = \begin{bmatrix} \dfrac{6\cot\alpha_i}{L_i^2} & 2\left(\dfrac{-\cos\theta_{1i}+\sin\theta_{1i}\cot\alpha_i}{L_i}\right) & 2\left(\dfrac{-\cos\theta_{2i}+\sin\theta_{2i}\cot\alpha_i}{L_i}\right) \\ \dfrac{-6\cot\beta_i}{L_{i+1}^2} & -2\left(\dfrac{\cos\theta_{1,i+1}+\sin\theta_{1,i+1}\cot\beta_i}{L_{i+1}}\right) & -2\left(\dfrac{\cos\theta_{2,i+1}+\sin\theta_{2,i+1}\cot\beta_i}{L_{i+1}}\right) \\ 6\left(\dfrac{1}{L_i^2}-\dfrac{1}{L_{i+1}^2}\right)\cot\gamma_i & 4f\,(\theta_{1i},\theta_{1,i+1},L_i,L_{i+1},\cot\gamma_i) & 4f\,(\theta_{2i},\theta_{2,i+1},L_i,L_{i+1},\cot\gamma_i) \end{bmatrix}, \tag{30}$$

where

$$f\,(\theta_i,\theta_{i+1},L_i,L_{i+1},\cot\gamma_i) = \left(\frac{\cos\theta_i}{L_i}+\frac{\cos\theta_{i+1}}{L_{i+1}}\right)+\left(\frac{\sin\theta_i}{L_i}-\frac{\sin\theta_{i+1}}{L_{i+1}}\right)\cot\gamma_i\,,$$

and

$$[\mathbf{C}_{ii}] = \left[\begin{array}{cccc|ccc} 1 & 1 & \cdots & 1 & -\cot\alpha_i & -\cot\alpha_i & \cdots & -\cot\alpha_i \\ 0 & 0 & \cdots & 0 & 0 & 0 & \cdots & 0 \\ -1 & 1 & \cdots & \pm 1 & \cot\gamma_i & -\cot\gamma_i & \cdots & \pm\cot\gamma_i \end{array}\right],$$

and

$$[\mathbf{C}_{i,i+1}] = \left[\begin{array}{cccc|ccc} 0 & 0 & \cdots & 0 & 0 & 0 & \cdots & 0 \\ 1 & 1 & \cdots & 1 & \cot\beta_i & \cot\beta_i & \cdots & \cot\beta_i \\ -1 & 1 & \cdots & \pm 1 & -\cot\gamma_i & \cot\gamma_i & \cdots & \pm\cot\gamma_i \end{array}\right].$$

3.1.2. Properties of the macro-element deduced from rank[C]

Row operations have been carried out algebraically with the aim of achieving a row echelon form. This has lead to the following general results as functions of p and n_Δ [6].

$p \geq 3$

Generally rank $[\mathbf{C}] = 3n_\Delta$ and there are no spurious kinematic modes for the assembly of primitives. The macro-element is hyperstatic and $n_{\text{hyp}} = \alpha - 3n_\Delta = 3 + n_\Delta\,(2p-4) + 0.5n_\Delta\,(p-2)\,(p-3)$. There is one exception when $n_\Delta = 4$ and the quadrilateral has a diagonal subdivision. Then rank $[\mathbf{C}] = 3n_\Delta - 1 = 12 - 1 = 11$, and the assembly contains 1 spurious mode and 1 extra hyperstatic mode. By inspection of the spurious modes of the primitives associated with the internal node of the macro-element, it is clear that these modes can be assembled to satisfy compatibility, and that the spurious mode for the assembly does not involve displacements of the external sides of the macro-element. Thus all tractions on the external sides remain admissible, and this "exceptional" case still presents a useful element. The presence of an extra hyperstatic mode may lead to lower levels of strain energy in a solution, an example is given when $p = 2$ when a similar situation occurs.

$p = 2$

A general result for $n_\Delta > 4$ requires further investigation, but for $n_\Delta = 3$ or 4 similar results hold as when $p = 3$, i.e. rank $[\mathbf{C}] = 3n_\Delta$, there are no spurious modes, and $n_{\text{hyp}} = 3 + n_\Delta\,(2p-4) = 3$. The exception again occurs for the quadrilateral with diagonal subdivision with similar consequences as when $p \geq 3$. The 4 hyperstatic modes which occur for a square element with diagonal subdivision are illustrated in Figure 9. It should be noted that if the geometry changes to a non-diagonal subdivision then mode 1 remains but modes 2 to 4 must be combined to give only two additional

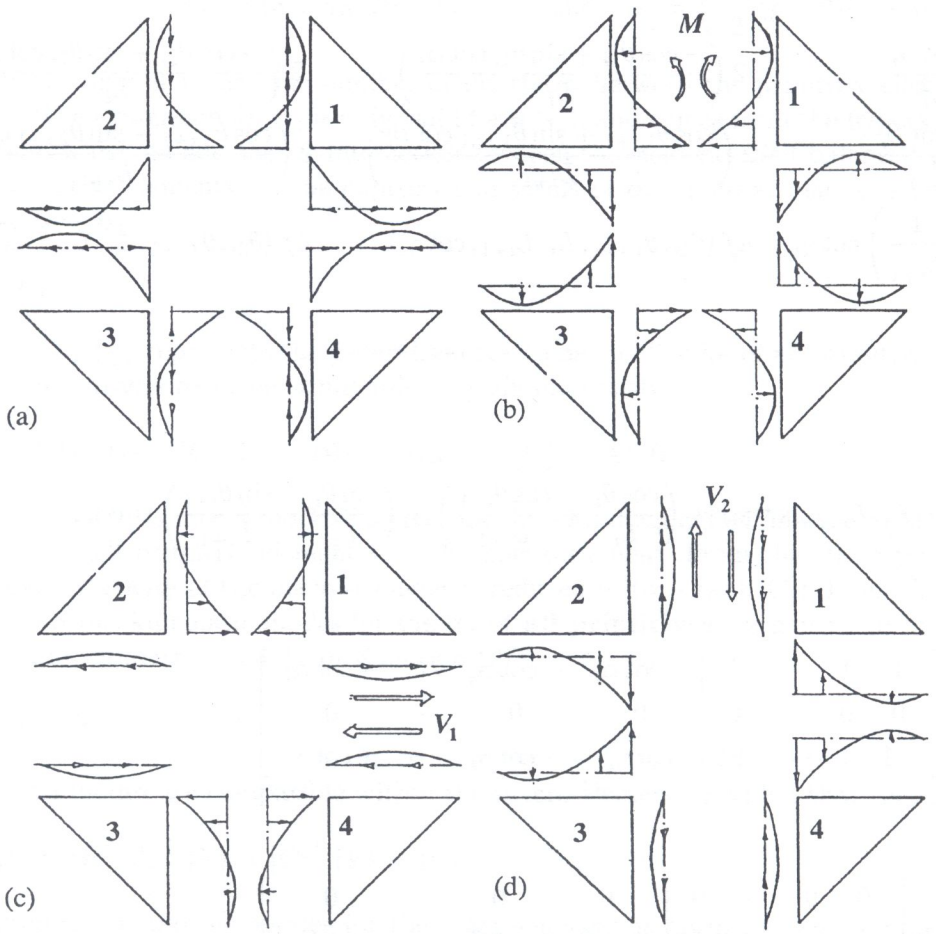

Fig. 9. Hyperstatic modes for a square macro-element with diagonal subdivision, $p = 2$: (a) mode 1, (b) mode 2, (c) mode 3, (d) mode 4

hyperstatic modes. The effect on the strain energy of a solution is illustrated in Figure 10 where strain energy is plotted as a function of the position of the internal node along the axis of symmetry. When the diagonal position D is reached there is a clear singularity in the energy function which

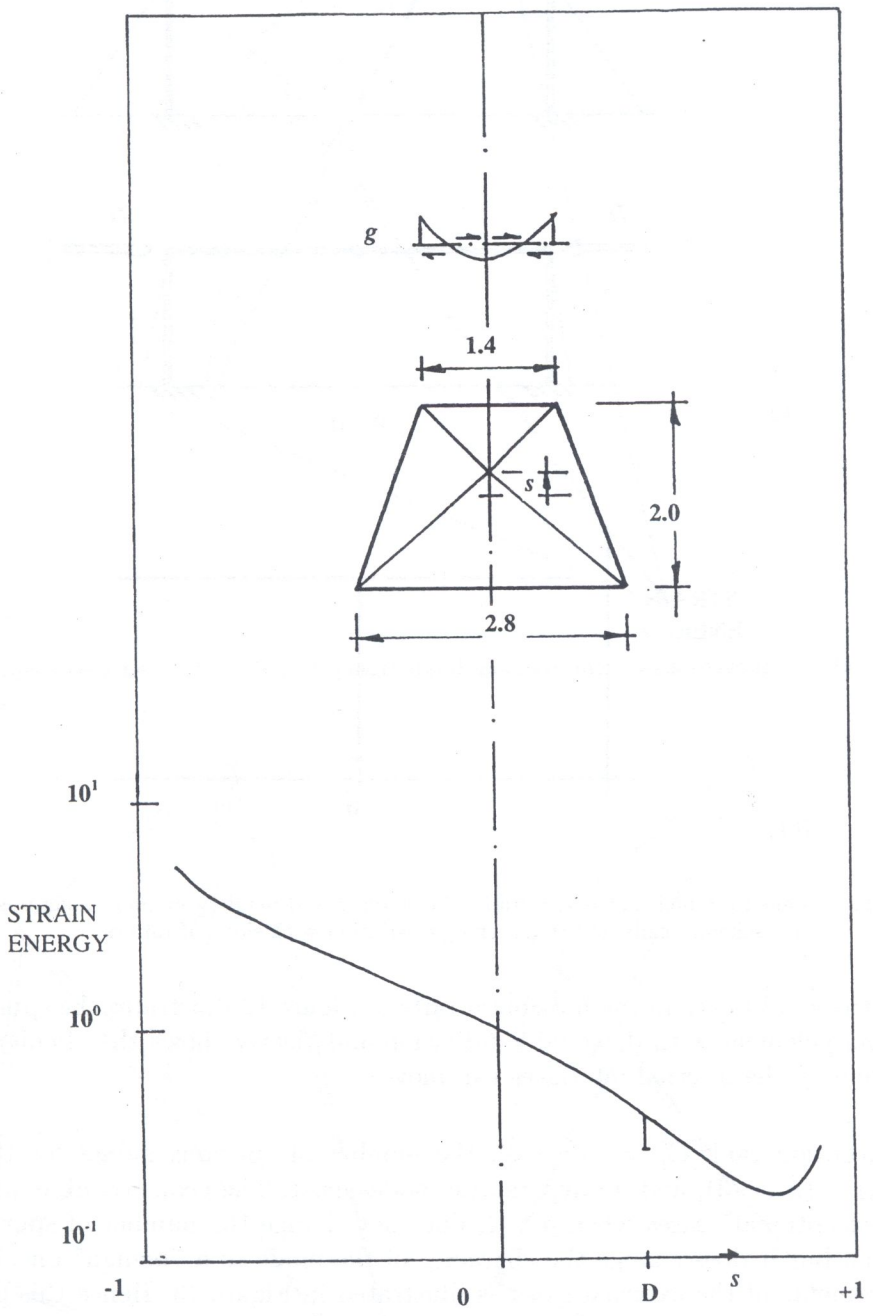

Fig. 10. Strain energy variation with position of the internal node, $p = 2$ and Poisson's ratio $\nu = 0.3$

is attributed to the additional hyperstatic mode. Similar singularities occur with simpler frame structures, and an example of a 3-pinned portal frame is shown in Figure 11. As the slope θ of the rafter is varied, so the strain energy due to a pair of horizontal forces H has a singularity when $\theta = 0$. When $\theta \neq 0$ the frame is isostatic, the strain energy is due solely to the bending of the columns, and is independent of θ. However, when $\theta = 0$ the frame becomes hyperstatic and contains one mechanism due to the alignment of the pin joints. The strain energy reduces to that

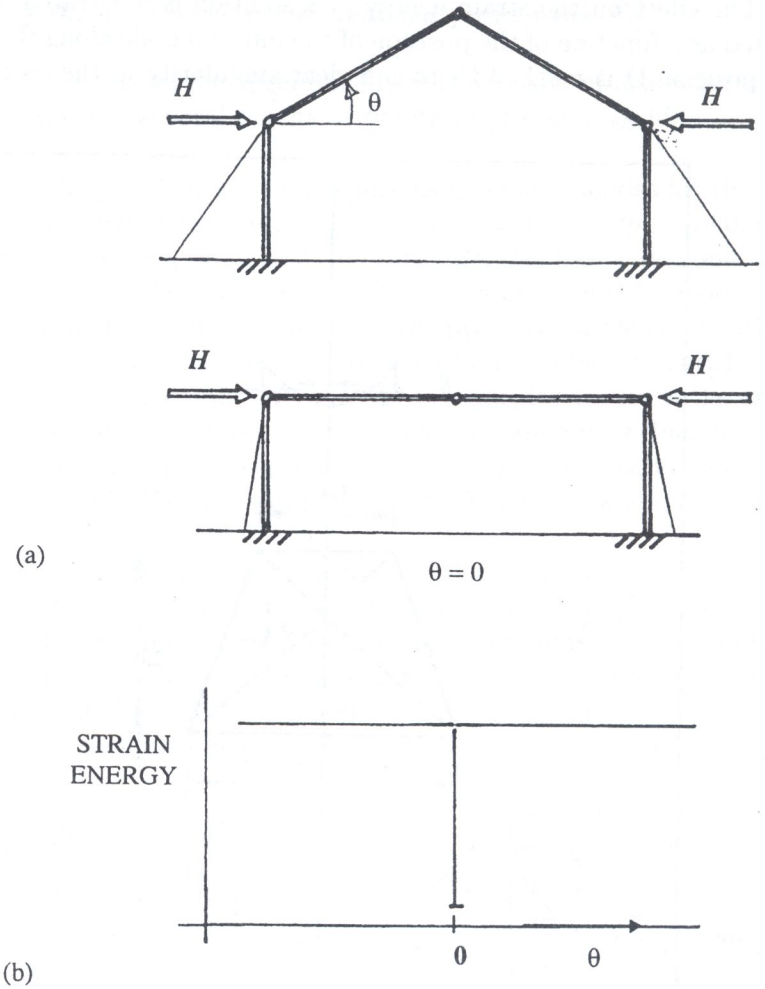

Fig. 11. 3 pinned pitched roof portal frame: (a) loading and bending moment diagrams shown schematically, (b) strain energy variation with slope of rafters

due mainly to the axial forces in the horizontal rafters. Figure 12 illustrates the spurious kinematic mode for a macro-element with diagonal subdivision and clearly shows the "benign" character of this mode since only the internal interfaces can move.

$p = 1$

Without exception $\text{rank}\,[\mathbf{C}] = (3 + n_\Delta)$, the number of spurious modes for the assembly is $2n_\Delta - (3 + n_\Delta) = (n_\Delta - 3)$, and no hyperstatic modes exist. The geometrical arrangement which leads to the "exceptional" cases when $p > 1$, does not change the number of spurious modes (in this case just 1), but it does change the character of the mode to a "benign" one, i.e. it does not involve displacements of the external sides as illustrated in Figure 13. Hence this geometry again presents a useful element.

3.1.3. General summary for a membrane macro-element with statically admissible stress fields

As the degree p of the polynomial fields increases so the problems with spurious kinematic modes are removed. The properties of macro-elements when viewed as single elements, and when effectively free of such modes, are summarised in Table 2.

Particular observations are included in Section 3.2 for the Trefftz type of element.

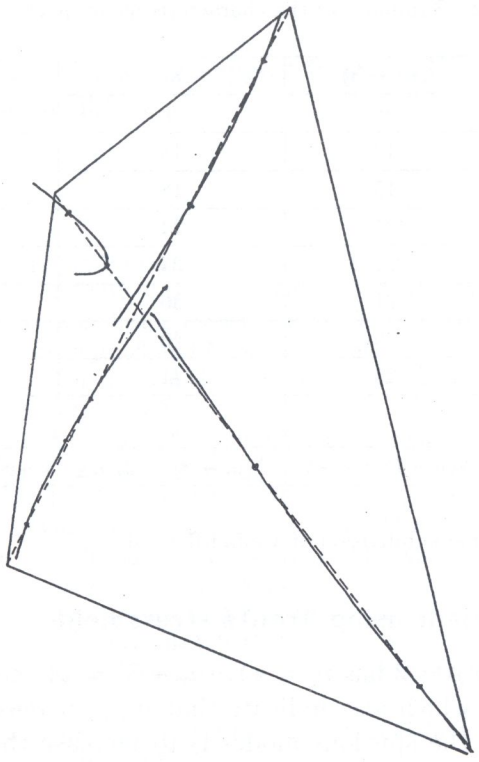

Fig. 12. Spurious kinematic mode of a quadrilateral macro-element with diagonal subdivision, $p = 2$.

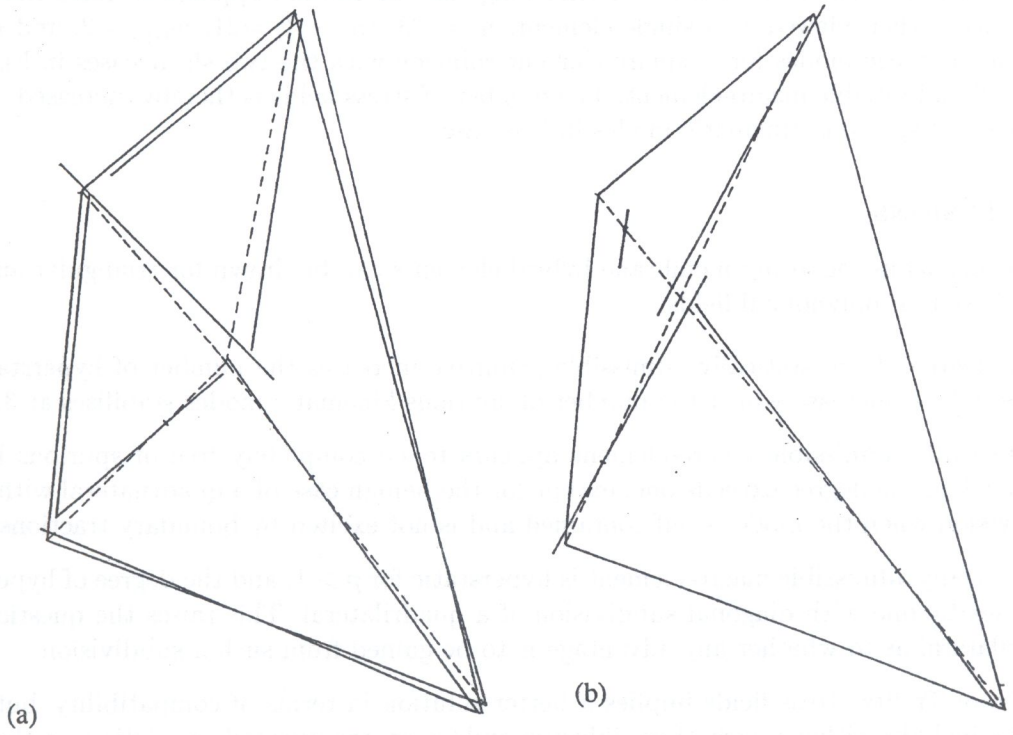

Fig. 13. Spurious kinematic modes of a quadrilateral macro-element with (a) non-diagonal and (b) diagonal subdivision, $p = 1$.

Table 2. Summary of the characteristics of macro-elements

Degree p	n_Δ	$(n_v - 3)$	n_s	n_{hyp}
1	3	9	9	0
1	4*	13	13	0
2	3	15	18	3
2	4	21	24	3
2	4*	21	25	4
3	3	21	30	9
3	4	29	40	11
3	4*	29	41	12
⋮	⋮	⋮	⋮	⋮
p	n_Δ	$2(p+1)\ n_\Delta - 3$	$\frac{1}{2}(p^2+3p+2)\ n_\Delta$	$\frac{1}{2}(p^2-p-2)\ n_\Delta + 3$

* indicates diagonal subdivision of a quadrilateral.

3.2. Membrane macro-element using Trefftz stress fields

A primitive quadrilateral with $p = 2$ has $n_s = 11$, $(n_v - 3) = 21$, $n_{hyp} = 0$, and $n_{skm} = 10$; this is confirmed by numerical trials which also indicate that n_{skm} increases by 4 for each unit increase of p. One way of coping with the spurious modes is to increase the degree of the internal stress fields relative to the degree of the displacement fields on the sides. However this may incur loss of equilibrium at element interfaces, and an alternative approach which could maintain equilibrium would be to formulate a macro-element based on Trefftz fields defined in a piecewise sense. A quadrilateral macro-element with $p = 2$ and diagonal subdivision appears to have the following characteristics when viewed as a single element: $n_s = 23$, $(n_v - 3)$ =21, $n_{hyp} = 2$, and $n_{skm} = 0$. The two hyperstatic modes for a square element coincide with the two shear cases in Figure 9 for the statically admissible macro-element. The number of stress fields is thereby increased, and there are no external spurious kinematic modes in this case.

4. Conclusions

General conclusions regarding membrane hybrid elements can be drawn for triangular and macro-elements based on polynomial fields:

- as the degree of the statically admissible primitive increases the number of hyperstatic stress fields tends to increase whilst the number of spurious kinematic modes stabilises at 3,
- the statically admissible macro-element appears to be completely free of spurious kinematic modes when the degree exceeds one, except for the benign case of a quadrilateral with diagonal subdivision when the mode is self contained and is not excited by boundary tractions,
- the statically admissible macro-element is hyperstatic for $p > 1$, and the degree of hyperstaticity increases by one with diagonal subdivision of a quadrilateral. This raises the question for the quadrilateral as to whether any advantage is to be gained from such a subdivision,
- the use of Trefftz stress fields implies a better solution in terms of compatibility, but the cost for this includes either a lack of equilibrium and/or an exaggerated restriction on the space of approximating functions. The errors and convergence rates of solutions obtained using statically admissible and Trefftz stress fields should be studied in detail,
- further work is required to establish general properties when Trefftz stress fields are used, and to extend similar studies to plate bending and solid elements.

ACKNOWLEDGEMENTS

The authors wish to express their thanks for support from the EC STRIDE Portugal programme which made their collaboration possible.

REFERENCES

[1] B.M. Fraeijs de Veubeke, G. Sander, P. Beckers. *Dual analysis by finite elements: linear and non linear applications.* Technical Report AFFDL-TR-72-93, Wright–Patterson Air Force Base, Ohio, 1972.

[2] B.M. Fraeijs de Veubeke. Diffusive equilibrium models. In: M. Geradin, ed., *B.M. Fraeijs de Veubeke Memorial Volume of Selected Papers*, 569–628. Sijthoff and Noordhoff, 1980.

[3] J. Jirousek, A. Venkatesh. Generation of optimal assumed stress expansions for hybrid–stress elements. *Computers and Structures*, **32**(6): 1413–1417, 1989.

[4] E.A.W. Maunder. A reappraisal of compound equilibrium finite elements. In: M.A. Erki, J. Kirkhope, eds., *Proceedings of the 12th Canadian Congress of Applied Mechanics*, 796–797. Carleton University, 1989.

[5] E.A.W. Maunder, J.P. Moitinho de Almeida, A.C.A. Ramsay. A general formulation of equilibrium macro–elements with control of spurious kinematic modes. *Int. J. Num. Meth. in Eng.*, **39**: 3175–3194, 1996.

[6] E.A.W. Maunder, J.P. Moitinho de Almeida. On the static and kinematic properties of 2-D hybrid equilibrium elements based on polynomials of degree p, (in preparation).

[7] J.P. Moitinho de Almeida, J.A. Teixeira de Freitas. Alternative approach to the formulation of hybrid equilibrium elements. *Computers and Structures*, **40**(4): 1043–1047, 1991.

[8] O.J.B. Pereira, J.P. Moitinho de Almeida. Automatic drawing of stress trajectories in plane systems. *Computers and Structures*, **53**: 473–476, 1994.

[9] A.C.A. Ramsay. *Robust variable degree equilibrium elements (formulation and application).* Report for Human, Capital and Mobility Network, ERB4050p1930382, 1995.

[10] J. Robinson. Equilibrium models. In: J. Robinson, ed., *State of the Art of Finite Element Methods in Structural Mechanics.* Robinson and Associates, 1975.

[11] J. Robinson. The mode amplitude technique and hierarchical stress elements — a simplified and natural approach. *Int. J. Num. Meth. in Eng.*, **21**: 487–507, 1985.